Revisiting the one-sided EWMA control chart

Article *in* International Journal of Applied Industrial Engineering · April 2022

DOI: 10.22105/JARIE.2021.301378.1369

3 authors:

Romina Dastoorian
Western Michigan University
12 PUBLICATIONS **73** CITATIONS
SEE PROFILE

Duy Duong-Tran
University of Pennsylvania
44 PUBLICATIONS **251** CITATIONS
SEE PROFILE

Lee J. Wells
Western Michigan University
56 PUBLICATIONS **1,323** CITATIONS
SEE PROFILE

E-ISSN: 2676-6167 | P-ISSN: 2538-5100

Journal of Applied Research on Industrial Engineering

www.journal-aprie.com

J. Appl. Res. Ind. Eng. Vol. 9, No. 2 (2022) 151–164.

Paper Type: Research Paper

Revisiting the One-Sided EWMA Control Chart

Duy Duong-Tran[1], Romina Dastoorian[2,*], Lee Wells[2]

[1] School of Industrial Engineering, Purdue University, United States; dduongtr@purdue.edu.

[2] Department of Industrial and Entrepreneurial Engineering and Engineering Management, Western Michigan University, United States; romina.dastoorian@wmich.edu; Lee.wells@wmich.edu.

Citation:

Duong-Tran, D., Dastoorian, R., & Wells, L. (2022). Revisiting the one-sided EWMA control chart. *Journal of applied research on industrial engineering, 9*(2), 151-164.

Received: 25/08/2021 Reviewed: 27/09/2021 Revised: 29/10/2021 Accepted: 04/12/2021

Abstract

Exponential Weighted Moving Average (EWMA) control charts have been widely used in Statistical Process Control (SPC) to detect small and persistent process shifts. In theory, EWMA control limits monotonically increase over time to account for the continual growth of the EWMA statistic's variance. However, these control limits are often assumed constant and are set to their respective asymptotic limits to simplify the process of applying and analyzing EWMA control charts. One-sided EWMA charts are often implemented when it is only desirable to detect shifts in a specific direction. When using one-sided EWMA charts, reflecting boundaries (resets) can be used to prevent the statistic from drifting too far from the chart's control limit, which can delay shift detection. There have been several research efforts into designing and studying the performance of one-sided EWMA charts with reflecting boundaries. However, these efforts have maintained the constant control limit assumption. When implementing a reflecting boundary, the EWMA statistic's variance is constantly being reset to zero, which may significantly affect the constant control limit assumption's validity. The focus of this paper is to understand behavior of the one-sided EWMA control charts with constant and time-varying limit assumption through simulation studies.

Keywords: ARL Performance, EWMA control charts, One-sided control charts, Quality control, Statistical process control.

1 | Introduction

With respect to control charts, the term 'one-sided' was noticeably mentioned by Roberts [1] for various control chart run/zone tests. Specifically, Roberts mentioned that there were "tests for runs up" and "for runs up and down". Later, various run/zone tests were studied, expressly, for the one-sided EWMA and CUSUM control charts by Roberts [2]. Despite mentioning one-sided control charts in both these publications, the focus was to study various run/zone tests for control charts rather than clearly defining the one-sided control chart and its statistical performance. Later, Lorden [3] and Brook and Evans [4] examined the performance of one-sided CUSUM versus traditional two-sided CUSUM control charts.

Corresponding Author: romina.dastoorian@wmich.edu

http://dx.doi.org/10.22105/jarie.2021.301378.1369

Robinson and Ho [5] and Crowder [6] considered one-sided control limits as a special design of EWMA control chart. Lucas and Saccucci [7] studied some features of EWMA control charts as fast initial responses for one-sided EWMA charts. Gan [8] explicitly defined the one-sided EWMA control chart and studied its performance using the Average Run Length metric. Although two-sided EWMA control charts attracted much more attention than its one-sided counterpart, Shu et al. [9] stated that the one-sided control chart has tremendous potential in rapidly detecting of upward or downward process shifts. For instance, in health surveillance, multivariate one-sided EWMA control charts have emerged as a competitive approach to monitor increases or decreases in disease outbreak rates and other medically related processes as mentioned by Joner Jr et al. [10]. However, all these mentioned efforts have maintained the constant control limit assumption when studied one-sided EWMA control charts. When implementing a reflecting boundary, the EWMA statistic's variance is constantly being reset to zero, which may significantly affect the constant control limit assumption's validity. The focus of this paper is to understand the impact of constant variance assumption on one-sided EWMA control chart's behavior. In this paper, we examine the performance of time-varying control limits versus constant control limits for one-sided EWMA control chart and one-sided combined Shewhart-EWMA chart.

The rest of this paper is organized as follows. In Section 2, a signal resistance simulation study demonstrates the statistical (dis)advantages of the constant limit one-sided EWMA control chart. In Section 3 and 4, ARL results and comparison analyses are presented for zero-state and steady-state, respectively. Final remarks and conclusion are presented in Section 5.

1.1 | One-Sided EWMA Control Charts

Control charts are usually considered as one of most powerfull tool of Statistical Process Control (SPC) and widely used in different applications and industry [11]-[13]. To introduce the one-sided EWMA, the EWMA needs to be introduced first. This paper focused on monitoring the mean of a process that generates independent observations of the random variable $X \sim N\left(\mu_0, \sigma_X^2\right)$ over time. For every observation of X at time (X_t), the EWMA statistic can be calculated as

$$Z_t = (1-\lambda)Z_{t-1} + \lambda X_t. \quad (1)$$

Where λ is the smoothing parameter $(0 < \lambda \leq 1)$ and $Z_0 = \mu_0$. The EWMA chart will issue an out-of-control signal if $Z_t < lcl_t$ or $Z_t > ucl_t$, where ucl_t, and lcl_t are the chart's upper and lower control limits at time t, respectively. These control limits can be calculated as

$$\mathrm{ucl}_t = \mu_0 + k\sigma_{Z_t}. \quad (2)$$

$$\mathrm{lcl}_t = \mu_0 - k\sigma_{Z_t}. \quad (3)$$

Where σ_{Z_t} is the standard deviation of Z_t and k is a design parameter to adjust control limit widths. As suggested by *Eqs. (2)* and *(3)* the standard deviation of the EWMA statistic is a function of time, which can be calculated as

$$\sigma_{Z_t} = \sigma_X \sqrt{\frac{\lambda[1-(1-\lambda)^{2t}]}{2-\lambda}}. \quad (4)$$

To simplify the process of applying and analyzing EWMA control charts, σ_{Z_t} is often assumed to be the constant

$$\sigma_Z = \lim_{t\to\infty} \sigma_X \sqrt{\frac{\lambda[1-(1-\lambda)^{2t}]}{2-\lambda}} = \sigma_X \sqrt{\frac{\lambda}{2-\lambda}}. \quad (5)$$

As a result of this assumption, the upper and lower control limits become the constants $ucl = \mu_0 + k\sigma_Z$ and $lcl = \mu_0 - k\sigma_Z$, respectively. While not theoretically correct, these constant control limits were assumed to have a minimal impact on the EWMA chart's performance.

One-sided EWMA charts are often implemented when it is only desirable to detect shifts in a specific direction. The upper one-sided EWMA statistic, which is a one-sided EWMA aimed at detecting positive shifts, with a reflecting boundary can be formulated as

$$Z_t = \max(A, (1-\lambda)Z_{t-1} + \lambda X_t. \quad (6)$$

Where the reflecting boundary, A, is a real value constant. The purpose of the reflecting boundary is to prevent Z_t from trending in the uninteresting direction. Using a constant control limit, an out-of-control signal is issued at the first sampling interval where $Z_t > ucl$. However, let t^* be the value of t when $(1-\lambda)Z_{t-1} + \lambda X_t < A$, which from *Eq. (6)* means that $Z_{t^*} = A$ and thusly $\sigma_{Z_{t^*}} = 0$. Therefore, when implementing theoretical time-varying control limits, the control limit should be reset to zero every time the reflecting boundary is triggered. This behavior of time-varying control limits is illustrated in *Fig. 1*. In *Fig. 1*, the EWMA statistic for sample 5 drops beneath the reflecting boundary, which triggers resetting both the EWMA statistic and the time-varying control limits at $t = 5$. It should also be noted that Gan [8] considered different values of Z_0 in his study, while in our study it was restricted to be $Z_0 = \mu_0$. It was due to the fact that this paper used time-varying control limit and having Z_0 above a control limit would result in an out of control observation at $t = 0$.

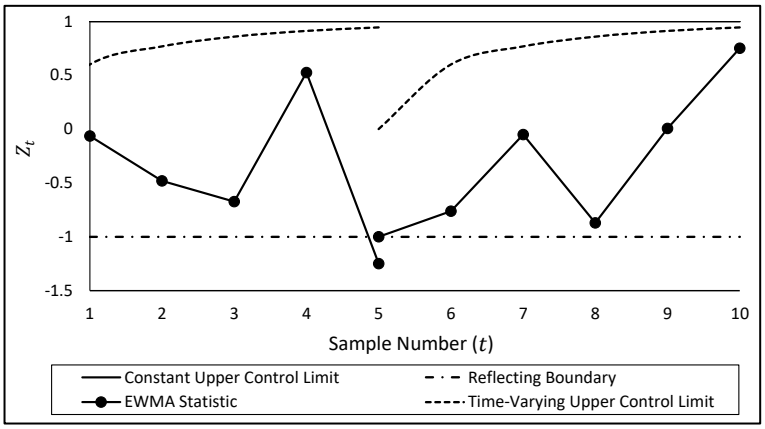

Fig. 1. EWMA control chart with constant and time-varying control limits.

Implementing constant limits with a reflecting boundary guarantees the maximum distance from the EWMA statistic to the control limit to be $ucl - A$. Similarly, charts with time-varying control limits with a relecting boundary guarantee the maximum distance from the EWMA statistic to the control limit to be $ucl_t - A$. Given that $ucl_t - A < ucl - A$ places constant control limit charts at a disadvantage as the EWMA statistic has further distance to travel to signal. In traditional two-sided EWMA charts, this fact is trivial since ucl_t converges to ucl rather quickly, resulting in very little performance differences. However, with the incorporation of a reflecting boundary with a one-sided EWMA, the EWMA statistic and ucl_t are constantly being reset. As a result of this resetting, the fact that ucl_t converges to ucl rather quickly may no longer be a sufficient reason to assume a constant control limit.

1.2 | Control Chart Performance

Control chart performances in this paper are measured based on the widely known metric Run Length, RL, which is defined as a number of sampling intervals necessary to detect the presence of a process shift. The shift size denoted as δ is a scalar multiple of the standard deviation of the control chart statistic. The Average Run Length hereby denoted as ARL is used in this paper is an evaluation criterion for comparing the performance of various control charts. There are three main numerical methods that are widely used to estimate ARL: Monte Carlo Simulation [1], discrete state Markov chain [4] and [7] and Fredholm integration quadrature [8], [14] and [15]. The presented ARL for various control charts in this paper are obtained from Monte Carlo simulations.

Control charts in this paper were simulated at both zero-state and steady-state. In zero-state, it is assumed that the shift introduced at the beginning of the process. In steady-state, it is assumed that the process has

been operating for some time before a process shift occurs. To investigate the effect of time-varying control limits on ARL performances, three one-sided control charts are considered and analyzed in this paper; namely: 1) one-sided EWMA with constant limits, 2) one-sided EWMA with time-varying limits, and 3) combined one-sided Shewhart-EWMA. All simulated ARL results for these control charts are provided in tabular form. To have a better visual perspective of ARL profiles, from here on, all Figs used to analyze ARL results are presented as the ratio of the ARL for a Shewhart chart to the ARL for the specific control chart being considered. This relative ARL performance, ARL*, is calculated as $ARL^* = \frac{ARL^S}{ARL^{scheme}}$, where ARL^{scheme} is the *ARL* of the control chart being considered. Larger ARL^* values indicate better performance and ARL^* values greater than one indicate that the chart outperforms a traditional Shewhart chart.

2 | Signal Resistance Simulation Study

Woodall and Mahmoud [16] used "signal resistance" to describe the inertia property of control charts and defined it as the "largest standardized deviation of sample mean from the target value not leading to an immediate out-of-control signal." In our paper, the signal resistances for one-sided EWMA charts with a reflecting boundary using constant limits and time-varying limits are explored. Specifically, a simulation study was performed to calculated signal resistances at time t for a one-sided constant limit EWMA chart (SR_t^C) and a one-sided time-varying limit EWMA chart (SR_t^T), as follow:

$$\mathrm{SR}_t^{\mathrm{C}} = \frac{\mathrm{ucl}-(1-\lambda)Z_t}{\lambda}.$$
$$\mathrm{SR}_t^{\mathrm{T}} = \frac{\mathrm{ucl}_t-(1-\lambda)Z_t}{\lambda}. \quad (7)$$

In this study, both control charts were tuned to have zero-state in-control *ARL* (ARL_0) equal to 500, which was obtained from 100,000 simulations. The inertia properties for 55 combinations of

$A = [0, -1]$ with -0.1 increments and $\lambda = [0.05, 0.25]$ with 0.05 increments were explored. Each combination of A and λ was simulated 10,000 times. For each simulation the constant and time-varying control charts were run simultaneously (both received the same random values $X \sim N(0, 1^2)$). Each simulation was terminated when either chart experienced 100 EWMA statistic resets or one of the two control charts provided an out-of-control signal. During the simulation, at each sampling interval, t, the difference between SR_t^C and SR_t^T was calculated as:

$$\mathrm{SR}_t = \mathrm{SR}_t^{\mathrm{T}} - \mathrm{SR}_t^{\mathrm{C}}. \quad (8)$$

At the end of each simulation the average signal resistance difference, $\overline{SR}$, was calculated. The grand average for signal resistance difference, $\overline{\overline{SR}}$, from all simulations were calculated for the 55 combinations of A and λ. These signal resistance results for $A = 0, -0.5, and\ -1$ are illustrated in *Fig. 2.a*. It should be noted, that in order to achieve equal in-control performances for the constant limit and time-varying limit control charts, for a given combination of A and λ, each chart's design parameter, k, is adjusted separately. As a result, $\lim_{t\to\infty} ucl_t > ucl$, or in other words at $t = 0$ the time-varying limit is beneath the constant limit and at some point in time (τ) they intersect resulting in the time-varying limit being above the constant limit. The time of intersection can be calculated as

$$\tau = \frac{\log\left(1-\left(\frac{k_c}{k_t}\right)^2\right)}{2\log(1-\lambda)}. \quad (9)$$

Where k_c and k_t are the design parameters for constant and time-varying limits, respectively. Time of intersection points for the signal resistance studies performed for $A = 0, -0.5, and\ -1$ are provided in *Fig. 2.b*.

Where k_c and k_t are the design parameters for constant and time-varying limits, respectively. Time of intersection points for the signal resistance studies performed for $A = 0, -0.5, and\ -1$ are provided in *Fig. 2.b.*

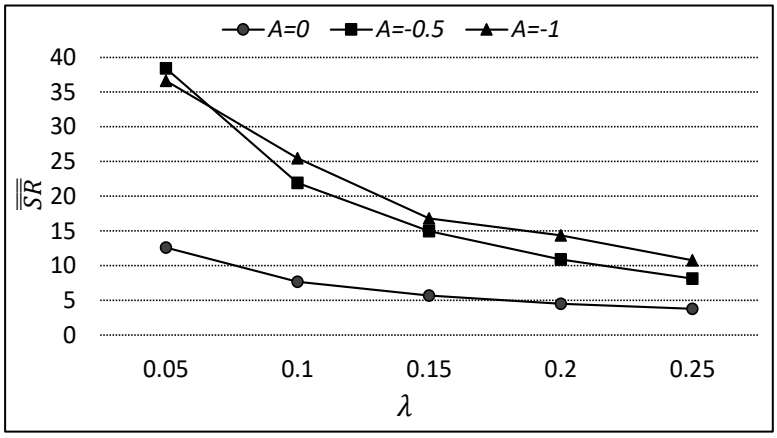

a.

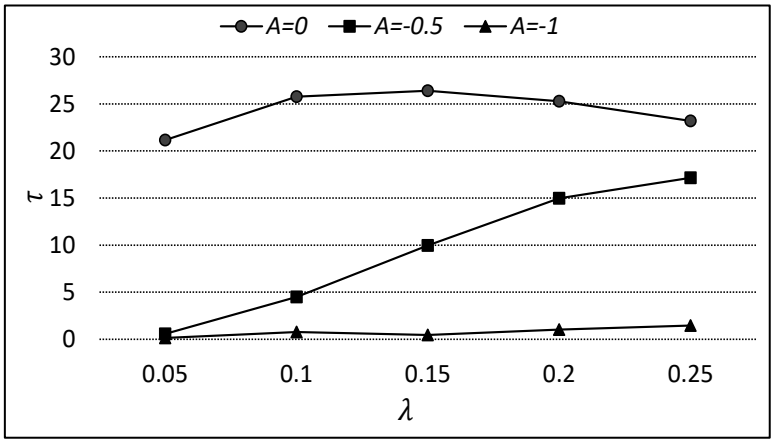

b.

Fig. 2. Signal resistance study results for; a. $\overline{\overline{SR}}$, b. τ for various combinations of A and λ.

In *Fig. 2.a*, positive $\overline{\overline{SR}}$ values indicate that the use of constant limits result in greater inertia compared to time-varying limit and therefore should have more difficulty signaling. As can be seen from *Fig. 2.a*, all combinations of A and λ have positive $\overline{\overline{SR}}$ values. These result are also consistent for the values of A that were excluded from *Fig. 2.a*. In addition, $\overline{\overline{SR}}$ tends to be larger for smaller values of $|A|$; and for larger values of $|A|$, $\overline{\overline{SR}}$ increases as λ increases. In addition, large $\overline{\overline{SR}}$ values tend to have small values of τ, as shown in *Fig. 2.b*. This means that the signal resistance of a constant limit control chart become worse (compared to time-varying limits) when the time-varying control limit quickly rises above the constant control limit (small τ). This suggests that the constant resetting of the EWMA statistic's variance drastically affects performance and urges a deeper investigation into the behavior of time-varying one-sided EWMA control charts.

3 | Zero-state ARL Analysis

In this section, zero-state ARL performances for constant and time-varying one-sided EWMA charts are simulated and analyzed. This simulation study covers the same combinations of A and λ discussed in Section 2.2. Also, as in Section 2.2, zero-state ARL_0 values are set to approximately 500 and are estimated from 100,000 simulations. The out-of-control ARL (ARL_1) performances for the charts are estimated using 100,000 simulations and compared over a wide spectrum of mean shifts ($\mu_1 = \mu_0 + \delta\sigma_X$) sizes. Specifically, simulated ARL_1 values are determined for δ values from 0 to 4 in increments of 0.1. For the sake of brevity, only a portion of these ARL_1 values are presented. Within each table, the smallest ARL_1 values for each

shift size are indicated by bold text. Furthermore, the smallest ARL_1 values for each shift size between both tables are underlined. To account for simulation error, if a ARL_1 value was within 1% of a bold or underlined ARL_1 (for a given shift size) it will also be bold or underlined, respectively.

Table 1. ARL zero-state constant limit one-sided EWMA.

		A=0			A=-0.2			A=-0.5			A=-1	
	λ	**0.05**	**0.15**	**0.25**	**0.05**	**0.15**	**0.25**	**0.05**	**0.15**	**0.25**	**0.05**	**0.15**	**0.25**
	k_c	**2.55**	**2.82**	**2.89**	**2.32**	**2.70**	**2.82**	**2.29**	**2.65**	**2.77**	**2.28**	**2.64**	**2.75**
δ	0	500.01	499.99	500.00	500.01	500.00	500.04	499.99	500.00	500.00	500.00	500.00	499.99
	0.2	95.06	128.97	155.32	82.96	118.06	143.78	80.18	110.67	138.74	79.75	110.02	136.36
	0.4	36.54	46.04	58.63	32.16	41.95	54.03	31.28	39.31	50.53	31.33	39.08	49.87
	0.6	20.74	22.51	27.40	18.64	20.74	25.45	18.20	19.74	24.04	18.22	19.58	23.66
	0.8	14.33	13.72	15.47	13.00	12.81	14.60	12.71	12.27	13.94	12.67	12.25	13.71
	1	10.95	9.60	10.14	9.94	9.04	9.63	9.74	8.78	9.26	9.72	8.72	9.16
	1.2	8.86	7.37	7.34	8.06	6.96	7.03	7.92	6.75	6.82	7.89	6.74	6.75
	1.4	7.45	5.97	5.73	6.80	5.68	5.52	6.67	5.52	5.35	6.68	5.49	5.31
	1.6	6.45	5.02	4.69	5.89	4.79	4.52	5.79	4.66	4.41	5.78	4.65	4.38
	1.8	5.69	4.34	3.97	5.20	4.14	3.84	5.13	4.05	3.75	5.10	4.03	3.74
	2	5.10	3.83	3.46	4.66	3.67	3.35	4.59	3.09	3.28	4.58	3.58	3.26
	2.5	4.08	3.00	2.65	3.74	2.88	2.57	3.69	2.82	2.54	3.68	2.82	2.52
	3	3.42	2.49	2.19	3.16	2.41	2.14	3.11	2.36	2.10	3.11	2.36	2.09
	4	2.63	1.97	1.67	2.41	1.91	1.62	2.37	1.88	1.59	2.37	1.88	1.58

Table 2. ARL zero-state time-varying limit one-sided EWMA.

		A=0			A=-0.2			A=-0.5			A=-1	
	λ	**0.05**	**0.15**	**0.25**	**0.05**	**0.15**	**0.25**	**0.05**	**0.15**	**0.25**	**0.05**	**0.15**	**0.25**
	k_c	**3.00**	**3.07**	**2.89**	**2.32**	**2.70**	**2.82**	**2.29**	**2.65**	**2.77**	**2.28**	**2.64**	**2.75**
δ	0	500.00	500.02	500.00	500.01	500.01	500.00	499.96	500.01	500.01	500.00	499.99	499.99
	0.2	132.76	164.23	184.90	77.90	124.38	155.50	72.27	109.06	139.90	72.41	107.65	135.06
	0.4	43.33	58.93	72.43	27.20	42.89	58.03	25.54	37.69	50.48	25.78	37.17	48.81
	0.6	20.98	26.46	32.94	14.08	20.19	26.35	13.28	18.05	23.48	13.35	17.90	22.71
	0.8	12.83	14.74	17.52	8.83	11.92	14.66	8.39	10.86	13.26	8.39	10.76	12.89
	1	8.79	9.75	10.91	6.14	7.99	9.34	5.84	7.36	8.57	5.86	7.33	8.39
	1.2	6.52	6.97	7.53	4.58	5.85	6.60	4.37	5.44	6.14	4.39	5.40	6.02
	1.4	5.06	5.35	5.63	3.60	4.51	5.01	3.45	4.24	4.67	3.46	4.22	4.59
	1.6	4.09	4.28	4.44	2.94	3.65	3.97	2.82	3.42	3.73	2.83	3.40	3.68
	1.8	3.41	3.54	3.62	2.48	3.04	3.28	2.38	2.87	3.08	2.38	2.84	3.04
	2	2.88	3.00	3.05	2.13	2.59	2.76	2.05	2.44	2.62	2.06	2.44	2.59
	2.5	2.07	2.14	2.16	1.59	1.88	1.98	1.55	1.79	1.89	1.55	1.78	1.87
	3	1.61	1.66	1.67	1.30	1.48	1.55	1.27	1.42	1.49	1.27	1.42	1.48
	4	1.16	1.18	1.19	1.05	1.11	1.14	1.05	1.09	1.11	1.05	1.09	1.11

As can been seen from the ARL results, a time-varying control limit chart always outperforms its constant control limit counterpart. However, for zero-state analysis, this result is not surprising since the time-varying control limit chart essentially has a head-start feature as the control limit at time $t = 1$ is rather close to μ_0. Another interesting result revolves around the ideal value for the reflecting boundary. Although Gan [8] suggested that $A = -1$ provides reasonable performance across the shift spectrum, our results show that reflecting boundaries from −0.5 to −1 also yield competitive ARL performances. This is evident in *Tables 1* and *2* where the performance at $A = -0.5$ and $A = -1$ show no noticeable differences. Finally, a very interesting behavior occurs with the performance of the time-varying control limit charts as a function of the smooth parameter (λ) value. Unlike other EWMA charts (e.g., constant control limit chart), the time-varying control limit chart tend to have superior performances for smaller λ across the shift spectrum. For instance, the best ARL performances ($A = -0.5$ and $A = -1$) all occur at $\lambda = 0.05$ regardless of the shift size.

A more important result from this analysis occurs when comparing the two control chart's performances with a Shewhart chart. The ARL^* performance profiles of both control charts for one specific reflecting boundary ($A = -0.5$) and two smoothing parameters ($\lambda = 0.05$ *and* 0.25) are presented in *Fig. 3*. It should be reemphasized that an ARL^* above 1 indicates superior performance compared to a Shewhart chart. Visibly, from *Fig. 3*, the ARL^* performances for the constant limit control chart were not consistently larger than 1 through the entire shift spectrum. This is not surprising as we expect to see superior performances from a Shewhart chart at large shift sizes. To the contrary, the time-varying

control limit has a ARL^* performance greater than 1 across the entire shift spectrum which makes it more competitive with the Shewhart at large shift sizes. It should be noted that this behavior occurs at all values of A that were analyzed. While this result is also somewhat trivial for zero-state, it does beg the need to investigate the steady-state behaviors of these two competing control charts.

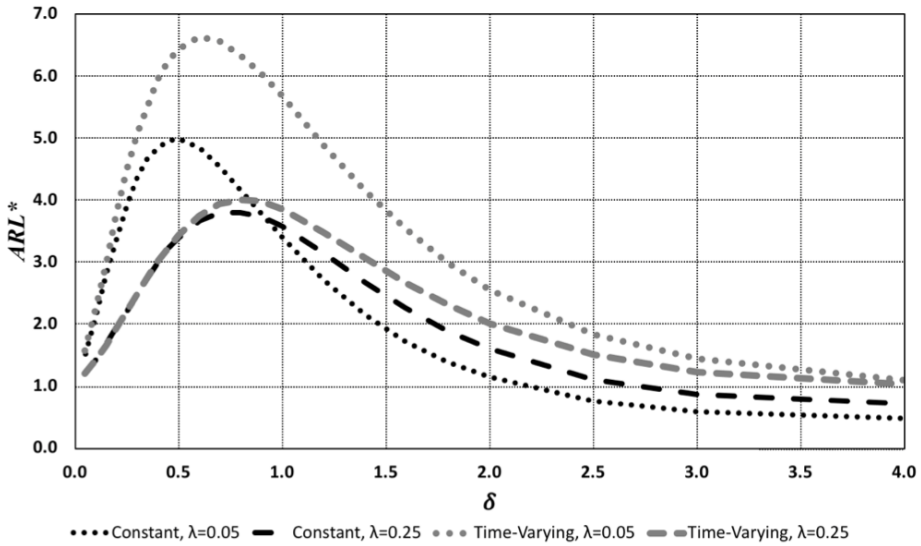

Fig. 3. Zero-state ARL* profiles for A = −0.5.

4 | Steady-State ARL Analysis

The results of Section 3 showed that for one-sided EWMAs, time-varying control limits offer superior zero-state performances over their constant limit counterparts. In this section, steady-state ARL performances for the two charts are simulated and analyzed. These steady-state simulations restrict the process to be in-control for the first 50 samples and introduce a sustained shift at sample 51. If any simulated control chart experiences a signal before sample 51 (i.e., false alarm), that simulation is disregarded. The steady-state ARL results of the simulation for constant and time-varying limits are represented in *Tables 3* and *4*, respectively. These tables follow the same syntax, with respect to bold and underlined ARL_1 values, as *Tables 1* and *2*.

Table 3. ARL results for steady-state constant limit one-sided EWMA.

		A=0			A=-0.2			A=-0.5			A=-1		
	λ	0.05	0.15	0.25	0.05	0.15	0.25	0.05	0.15	0.25	0.05	0.15	0.25
	k_c	2.56	2.82	2.90	2.33	2.71	2.82	2.29	2.65	2.77	2.29	2.65	2.75
δ	0	499.84	500.04	499.84	499.77	499.93	500.06	500.38	500.11	499.81	500.00	500.01	500.02
	0.2	89.46	126.56	153.43	80.46	116.37	145.92	78.98	110.67	136.79	79.15	109.55	135.73
	0.4	32.15	44.04	57.22	31.01	40.74	53.15	31.02	38.88	49.89	31.18	38.48	49.20
	0.6	17.60	20.91	26.22	17.96	19.80	24.67	18.23	19.33	23.53	18.27	19.37	23.25
	0.8	11.88	12.36	14.50	12.48	12.12	13.93	12.80	12.08	13.54	12.80	12.08	13.47
	1	8.98	8.52	9.33	9.61	8.50	9.12	9.85	8.57	9.00	9.87	8.63	9.03
	1.2	7.18	6.41	6.70	7.82	6.51	6.62	8.04	6.65	6.60	8.04	6.66	6.65
	1.4	6.03	5.17	5.14	6.57	5.29	5.16	6.79	5.42	5.19	6.80	5.44	5.24
	1.6	5.18	4.31	4.20	5.71	4.46	4.22	5.90	4.59	4.28	5.91	4.62	4.31
	1.8	4.56	3.72	3.53	5.06	3.86	3.58	5.24	4.00	3.65	5.24	4.01	3.69
	2	4.09	3.28	3.06	4.53	3.42	3.12	4.70	3.53	3.18	4.71	3.57	3.22
	2.5	3.27	2.56	2.32	3.64	2.69	2.39	3.78	2.79	2.45	3.78	2.82	2.49
	3	2.75	2.13	1.91	3.08	2.24	1.98	3.19	2.33	2.03	3.20	2.36	2.06
	4	2.13	1.67	1.44	2.39	1.74	1.51	2.48	1.81	1.56	2.49	1.83	1.58

Table 4. ARL results for steady-state time-varying limit one-sided EWMA.

		A=0			A=-0.2			A=-0.5			A=-1		
	λ	0.05	0.15	0.25	0.05	0.15	0.25	0.05	0.15	0.25	0.05	0.15	0.25
	K_T	3.00	3.08	3.08	2.37	2.77	2.88	2.29	2.66	2.78	2.29	2.64	2.75
δ	0	500.00	499.98	499.98	500.00	500.00	500.00	500.01	500.01	499.99	500.00	500.00	500.00
	0.2	133.36	164.00	183.95	82.33	124.48	155.16	78.64	111.35	139.20	79.07	109.03	135.24
	0.4	42.43	58.16	72.18	31.14	42.98	57.44	31.00	39.08	51.11	30.98	38.49	49.25
	0.6	20.70	25.82	32.26	17.81	20.59	26.30	18.28	19.35	23.85	18.30	19.28	23.38
	0.8	12.88	14.31	17.18	12.28	12.33	14.62	12.82	12.04	13.60	12.80	12.03	13.46
	1	9.11	9.35	10.57	9.33	8.54	9.42	9.82	8.55	9.03	9.86	8.60	9.00
	1.2	7.03	6.78	7.27	7.53	6.45	6.72	8.06	6.60	6.61	8.04	6.66	6.64
	1.4	5.69	5.27	5.45	6.32	5.18	5.19	6.79	5.38	5.19	6.81	5.45	5.23
	1.6	4.76	4.28	4.31	5.47	4.32	4.19	5.90	4.54	4.25	5.93	4.60	4.31
	1.8	4.10	3.61	3.55	4.80	3.73	3.53	5.23	3.96	3.62	5.25	4.01	3.68
	2	3.61	3.12	3.02	4.30	3.27	3.05	4.69	3.51	3.16	4.71	3.56	3.22
	2.5	2.79	2.34	2.21	3.44	2.52	2.29	3.78	2.76	2.42	3.79	2.82	2.49
	3	2.30	1.89	1.76	2.89	2.09	1.86	3.19	2.31	1.99	3.20	2.36	2.06
	4	1.75	1.40	1.28	2.23	1.59	1.37	2.47	1.78	1.51	2.48	1.82	1.58

From these results several interesting behaviors can be seen. Firstly, Gan [8] suggested that $A = -1$ provides good performance; however, this does not appear to be the case in steady-state. In fact, $A = -1$ results in the worst performances for the majority of the shifts considered and only provided slightly better results for small shifts. In general, for both constant and time-varying limit control charts, the closer the reflecting boundary (A) gets to zero the better the performance with detecting large shifts. Furthermore $A = 0$ and $A = -0.2$ seem to provide more robust performances for the constant and time-varying control charts, respectively. When comparing the best ARL_1 values (for each shift size), obtained from the two charts, there is very little difference.

To assist in the comparison between constant and time-varying limit control charts, their ARL^* performance profiles for two reflecting boundaries, $A = 0$ and -0.2, and two smoothing parameters ($\lambda = 0.05$ *and* 0.25) are presented in *Fig. 4*. This figure shows for the same values of A and λ, the constant limit chart tends to perform significantly better for smaller shifts. On the other hand, for large shifts, time-varying performs better; but not significantly better. Moreover, as λ increases the shift size at which the performances switch (constant and time-varying profiles intersect) increases. Also, as $|A|$ increases the performances of the two charts begin to converge. This is to be expected, since as $|A|$ increases the one-sided EWMA statistic will be reset less often. This is also the reason for only providing ARL^* performance profiles for $A = 0$ and -0.2, as other values of A the performances between constant and time-varying are not visually discernable.

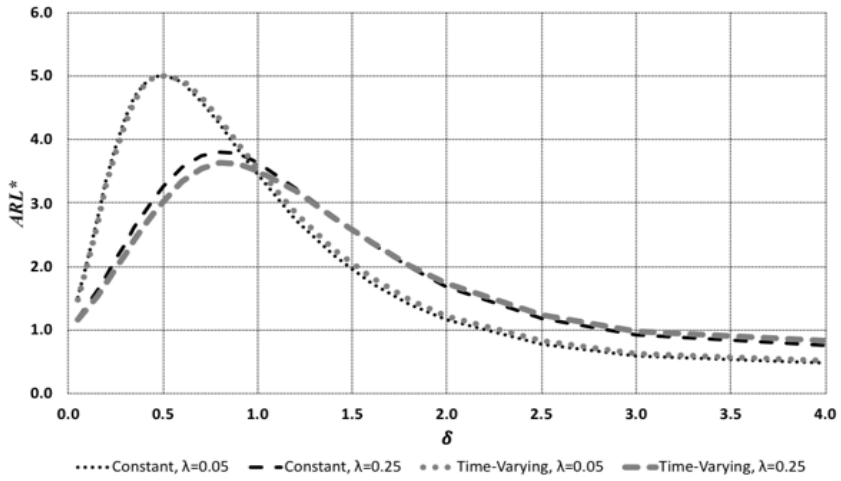

a.

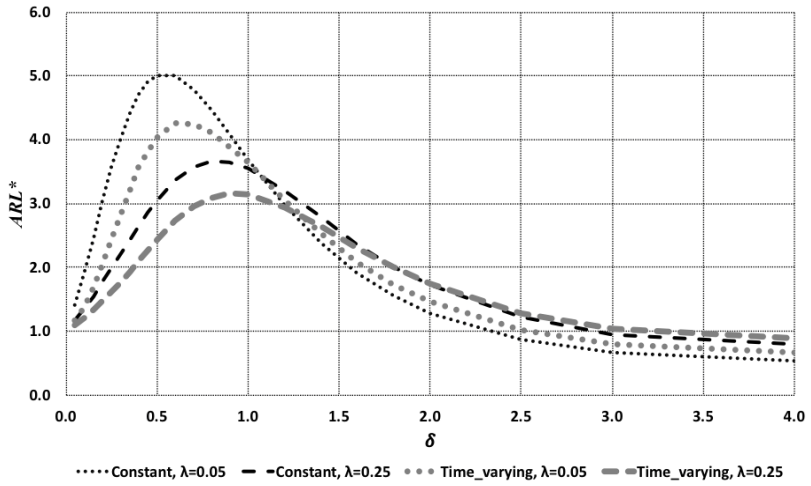

b.

Fig. 4. Steady state ARL* profiles for; a. A = 0 , b. A = −0. 2.

4.1 | One-sided Combined Shewhart Chart

In Lucas and Saccucci [7], the Combined Shewhart-EWMA (CSEWMA) was mentioned as a control chart with reasonable performance towards detecting both small and large shift sizes. More recently, Capizzi and Masarotto [17] studied the behavior of CSEWMA with estimated parameters. Given that the one-sided EWMA with time varying limits showed good steady-state performance for both small (Compared to a Shewhart) and large shifts (compared to the constant limit one-sided EWMA), in our paper we compare its performance to a one-sided CSEWMA with a reflecting boundary set to zero. Besides the required parameters to simulate the one-sided CSEWMA such as k_S (Shewhart chart parameter), k_C, and λ one usually introduces an extra parameter $R = ARL_0^S/ARL_0^C$ to express a specific interest in detecting shift sizes range. By changing the value of R, one can adjust the weights placed on the two control charts. For instance, $R = 1$ sets equal weight to both control charts. Setting $R > 1$ implies more emphasis is placed on the EWMA chart (i.e., EWMA signals easier than Shewhart) and is therefore more sensitive to smaller shifts. Lastly, $R < 1$ provides better performance in detecting large shifts by placing more emphasis on the Shewhart chart. The parameter $R \cong 2$, $R \cong 1$, and $R \cong 0.3$ were selected to represent three different CSEWMA designs. *Table 5* presents the *ARL* results for these three CSEWMA designs. Within *Table 5*, the smallest ARL_1 values for each shift size are indicated by bold text. Furthermore, if a bold ARL_1 value in *Table 5* is less than its counterpart in *Table 4* (steady-state time-varying limit) it is underlined. To account for simulation error, if a ARL_1 value was within 1% of a bold or underlined ARL_1 (for a given shift size) it will also be bold or underlined, respectively. Finally, if a bold ARL_1 value in *Table 5* is within 1% of a bold ARL_1 value in *Table 4* (for a given shift size) it is double underlined.

Table 5. ARL results for steady-state one-sided CSEWMA.

		R≈2			**R≈1**			**R≈0.3**		
	λ	**0.05**	**0.15**	**0.25**	**0.05**	**0.15**	**0.25**	**0.05**	**0.15**	**0.25**
	K_s	**3.20**	**3.18**	**3.18**	**2.81**	**3.01**	**3.05**	**3.01**	**2.95**	**2.94**
	K_{EWMA}	**2.71**	**2.95**	**3.00**	**3.08**	**3.09**	**3.09**	**3.09**	**3.29**	**3.32**
δ	0	499.99	499.95	499.99	500.03	499.99	499.93	500.04	500.04	499.97
	0.2	100.95	142.72	168.72	110.36	152.14	178.04	134.66	188.55	216.23
	0.4	35.28	50.04	64.07	37.94	53.82	68.91	44.63	69.55	91.15
	0.6	18.95	23.09	28.98	20.07	24.44	31.06	22.75	30.38	41.04
	0.8	12.59	13.43	15.86	13.14	14.01	16.67	14.55	16.56	21.34
	1	9.34	9.06	10.01	9.68	9.35	10.43	10.58	10.66	12.55
	1.2	7.38	6.73	7.06	7.63	6.94	7.29	8.18	7.74	8.47
	1.4	6.08	5.33	5.36	6.24	5.43	5.48	6.57	5.92	6.22
	1.6	5.11	4.39	4.29	5.19	4.46	4.39	5.45	4.78	4.83
	1.8	4.39	3.71	3.58	4.42	3.77	3.62	4.54	3.97	3.90
	2	3.80	3.21	3.05	3.79	3.23	3.08	3.84	3.36	3.27
	2.5	2.73	2.36	2.22	2.64	2.33	2.21	2.60	2.35	2.27
	3	2.00	1.81	1.72	1.91	1.77	1.70	1.83	1.74	1.69
	4	1.24	1.22	1.20	1.20	1.19	1.18	1.17	1.16	1.16

Naturally, $R \cong 2$ shows superior for small shift sizes (more emphasis on EWMA chart) and $R \cong 0.3$ was superior for large shift sizes (more emphasis on Shewhart chart). However, it can be seen that $R \cong 2$ gave the best overall results across the shift spectrum, as the differences in performances for large shifts were negligible and for small shifts were significant. Therefore, for brevity, we will focus on comparing time-varying performances to CSEWMA for $R \cong 2$. The ARL^* performance profiles for the time-varying control chart with $A = 0$ and -0.2 and the CSEWMA with $R \cong 2$ are given in *Fig. 5* for $\lambda = 0.05$ *and* 0.25.

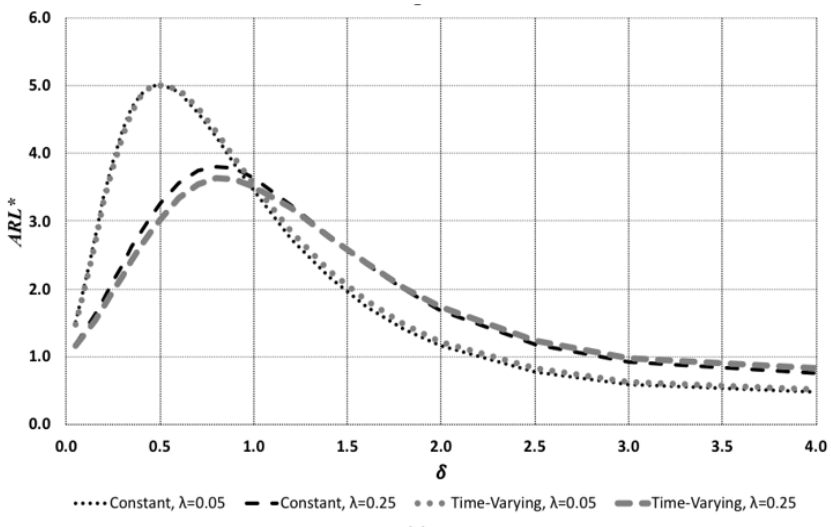

a.

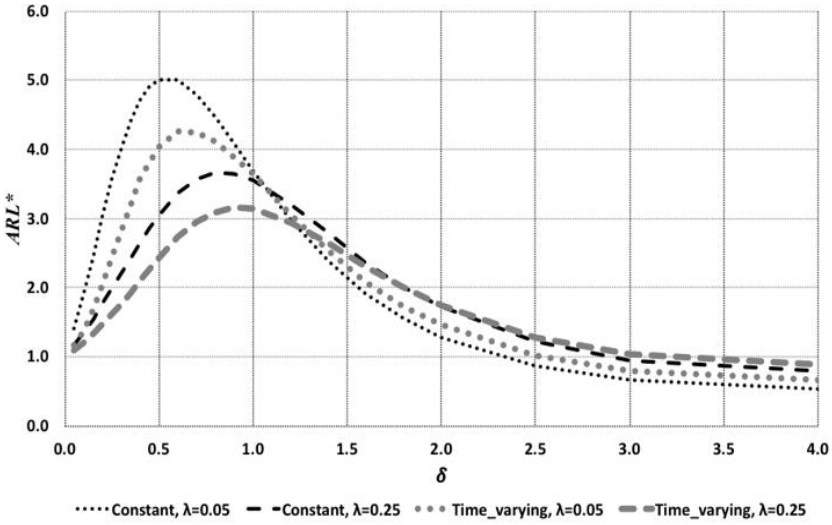

b.

Fig. 5. Steady state ARL* profiles for time-varying and CSEWMA with R ≅ 2 for; a. A = 0 , b. A = −0. 2.

Before discussing *Fig. 5* it should be mentioned that the CSEWMA results for *Fig. 5.a* and *5.b* are the same and that the differences are in the time-varying results. When $A = 0$, for a given value of λ, it appears that the CSEWMA outperforms for small and large shifts and underperforms for medium size shifts compared to the time-varying limit control chart. As can be seen in *Fig. 5.b*, as $|A|$ increases this behavior transitions to the time-varying control chart performing better than the CSEWMA for smaller shifts. There is no need to consider the behavior for larger values of $|A|$ as this trend will continue since larger values of $|A|$ are better for smaller shifts and worse for larger ones. For similar reasons, there is little reason to consider smaller R values, which will result in CSEWMAs that perform even better for larger shifts and worse for smaller shifts. In summary, it does not appear that the time-varying limit chart can outperform the CSEWMA for large shifts. This is especially true considering that, for *Fig. 5*, the best time-varying limit charts for large shifts were chosen ($|A|$ was close to zero) and the worst CSEWMA for large shifts was chosen ($R \cong 2$).

4.2 | Impact of Process Shift

The performance of the one-sided control charts, that have been analyzed, vary over the shift spectrum. In general, for the same values of λ, the constant limit control chart performs best for small shifts; the time-varying limit control chart performs best for medium shifts, and the CSEWMA performs best for large shifts. Therefore, if the shift magnitudes and costs are known to practitioners, choosing the optimal scheme is rather straightforward. However, this is not realistic in most cases. To investigate the impact of unknown shift sizes on control charting performance, a weighting function for shift sizes $\left(f(\delta)\right)$ is considered. For each control chart considered in this paper, a weighted ARL_1 performance,

$$\mathrm{ARL}_1^{\mathrm{w}} = \int_0^4 \mathrm{ARL}_1(\delta)\mathrm{f}(\delta)\mathrm{d}\delta. \tag{10}$$

Is calculated via numerical integration (trapezoid) using steady-state ARL_1 performance results (including shift sizes that were omitted from the tables). For this study, a Beta distribution was chosen for $f(\delta)$. To cover a wide range of shift size weighting functions, six different combinations of the Beta distribution's parameters (α, β) were considered. These six different weighting functions are illustrated in *Fig. 6*.

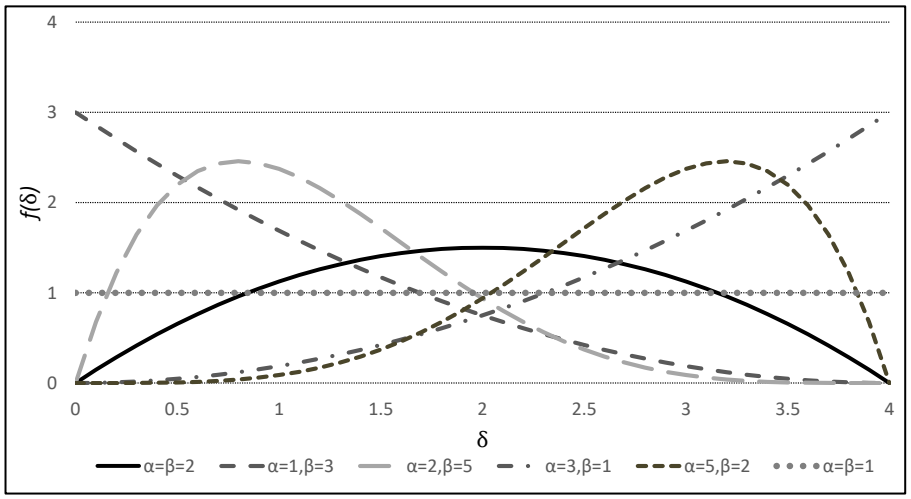

Fig. 6. Shift size weighting functions.

For each weighting function, the control chart scheme (combination of design parameters) with the best (smallest) ARL_1^w were determined for each of the three control charts considered in this paper. The results of this analysis are provided in *Table 6*, where charts are listed in order of the best, middle, and worst performing charts; with respect to their minimum ARL_1^w. In addition, the parameters for each control chart type that resulted in the minimal ARL_1^w are provided. Lastly, the ARL_1^w percent differences, with respect to the best performing charts minimal ARL_1^w are provided. For instance, for $(\alpha = 2, \beta = 2)$ the overall best performing chart was a time-varying (T) limit chart with a $ARL_1^w = 29.60$, which occurred when $A = -0.1$ and $\lambda = 0.05$. The middle performing chart was a constant (C) limit chart with an $ARL_1^w = 29.80$ (0.68% different from 29.60), which occurred when $A = -0.2$ and $\lambda = 0.1$. The worst performing chart was a CSEWMA (CS) chart with an $ARL_1^w = 30.28$ (2.30% different from 29.60), which occurred when $R \cong 2$ and $\lambda = 0.05$.

Table 6. Optimal weighted ARL_1 performances.

α,β	2,2	1,3	2,5	3,1	5,2	1,1
Best	29.60 (T) A=-0.1; λ=0.05	122.18 (C) A=-0.2; λ=0.05	68.15 (T) A=-0.2; λ=0.05	9.42 (CS) R≈2; λ=0.2	7.81 (CS) R≈2; λ=0.25	56.07 (C) A=-0.7; λ=0.05
Middle	29.80 (C); 0.68% A=-0.2; λ=0.1	122.40 (T); 0.18% A=-0.7; λ=0.05	68.17 (C);0.03% A=-0.2; λ=0.05	9.72 (T); 3.18% A=-0.1; λ=0.25	7.90 (T); 1.15% A=0; λ=0.25	56.12 (T); 0.09% A=-0.3; λ=0.05
Worst	30.28 (CS);2.30% R≈2; λ=0.05	143.55 (CS);17.49% R≈2; λ=0.05	7500 (CS); 10.05% R≈2; λ=0.05	9.94 (C); 5.52% A=0; λ=0.25	8.17 (C); 4.61% A=0; λ=0.25	61.32 (CS);9.36% R≈2; λ=0.05

From *Table 6* it can be seen that the time-varying limit control chart (bolded) is either the best or second best (middle) and is never the worst performing control chart for the 6 different weighting functions considered. Furthermore, the percent difference for the middle performing chart is always significantly less than the percent difference for the worst performing chart. In other words, the performance of the time-varying limit control chart is never the worse, and when it is the second best (middle) it is much better than the worst. From this analysis, it can be stated that the one-sided time-varying limit EWMA control chart provides very robust performances when the distribution (or cost) of different shift sizes is unknown or highly difficult to estimate. Lastly, to aid in the design of a one-sided time-varying limit EWMA control chart, steady-state ARL_1^w performances are provided as contour plots in *Fig. 7* for three combinations of α and β.

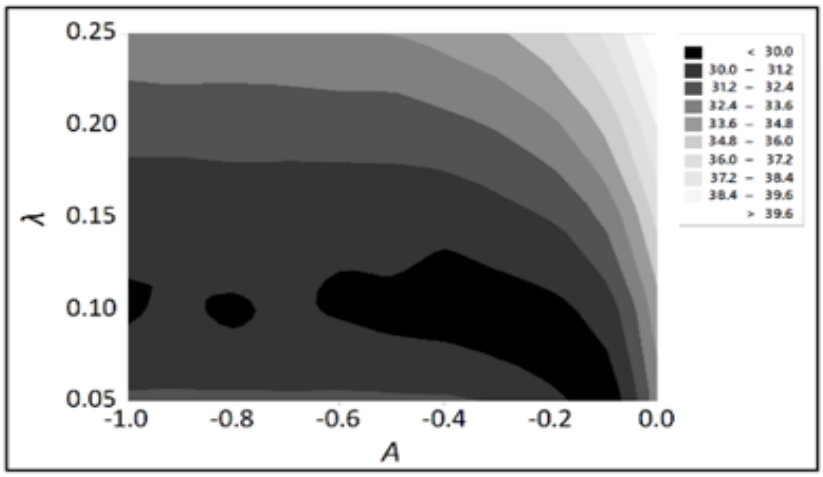

a.

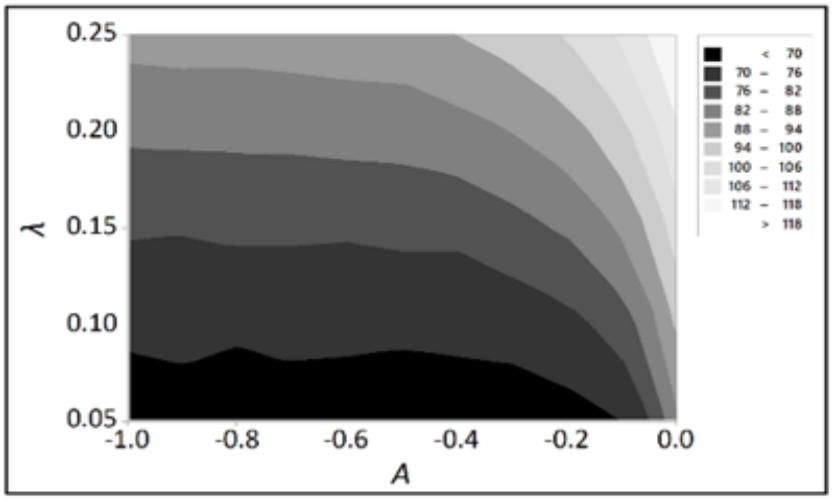

b.

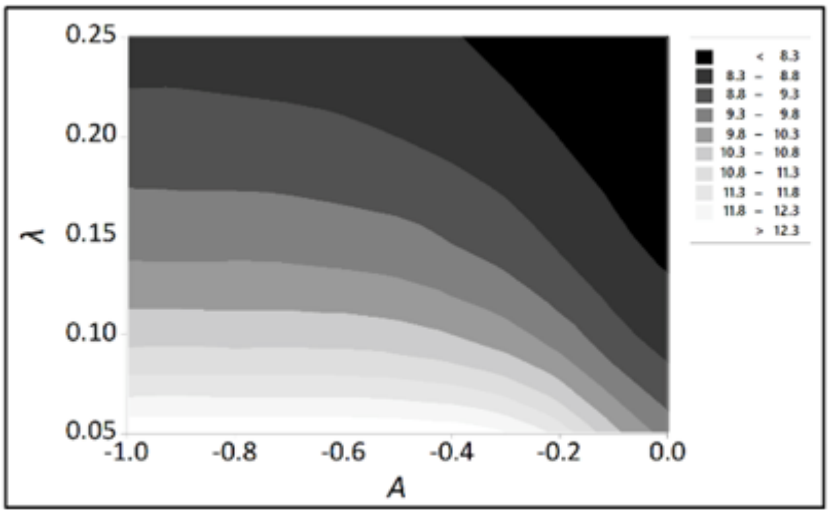

c.

Fig. 7. Weighted ARL_1 performances for weighting functions: a. $\alpha = \beta = 2$; b. $\alpha = 2$, $\beta = 5$, c. $\alpha = 5$ and $\beta = 2$.

5 | Conclusion and Future Reserach

The purpose of this paper was to investigate the impact of a constant variance on the performance of one-sided EWMA control chart. For zero-state, the use of time-varying control limits showed superior performances, with respect to constant limit one-sided EWMA and Shewhart charts, across the shift spectrum. Steady-state analysis showed that time-varying control limit charts outperform their constant limit counterparts for large shifts but underperform for small shifts. Given this performance behavior, the time-varying limit chart was compared to the one-sided combined Shewhart-EWMA (CSEWMA) chart in steady-state. In general, the time-varying limit chart performed better than the CSEWMA for smaller shifts, which means that it best for medium sized shifts (compared to CSEWMA and constant limit charts). Considering all three charts, further results demonstrated that the time-varying control chart is either the best or second best (never the worst) when considering different shift size distributions (weights). In conclusion, the one-sided time-varying control limit EWMA chart should be considered when the cost or distribution of shift sizes is unknown or difficult to estimate.

Funding

There was no funding for this research.

Conflicts of Interest

There is no financial interest to report.

References

[1] Roberts, S. W. (1958). Properties of control chart zone tests. *Bell system technical journal*, *37*(1), 83-114.

[2] Roberts, S. W. (1966). A comparison of some control chart procedures. *Technometrics*, *8*(3), 411-430.

[3] Lorden, G. (1971). Procedures for reacting to a change in distribution. *The annals of mathematical statistics*, *42*(6), 1897-1908.

[4] Brook, D. A. E. D., & Evans, D. (1972). An approach to the probability distribution of CUSUM run length. *Biometrika*, *59*(3), 539-549.

[5] Robinson, P. B., & Ho, T. Y. (1978). Average run lengths of geometric moving average charts by numerical methods. *Technometrics*, *20*(1), 85-93.

[6] Crowder, S. V. (1987). A simple method for studying run–length distributions of exponentially weighted moving average charts. *Technometrics*, *29*(4), 401-407.

[7] Lucas, J. M., & Saccucci, M. S. (1990). Exponentially weighted moving average control schemes: properties and enhancements. *Technometrics*, *32*(1), 1-12.

[8] Gan, F. F. (1993). Exponentially weighted moving average control charts with reflecting boundaries. *Journal of statistical computation and simulation*, *46*(1-2), 45-67.

[9] Shu, L., Jiang, W., & Wu, S. (2007). A one-sided EWMA control chart for monitoring process means. *Communications in statistics—simulation and computation®*, *36*(4), 901-920.

[10] Joner Jr, M. D., Woodall, W. H., Reynolds Jr, M. R., & Fricker Jr, R. D. (2008). A one-sided MEWMA chart for health surveillance. *Quality and reliability engineering international*, *24*(5), 503-518.

[11] Gol-Ahmadi, N., & Raissi, S. (2018). Residual lifetime prediction for multi-state system using control charts to monitor affecting noise factor on deterioration process. *Journal of applied research on industrial engineering*, *5*(1), 27-38.

[12] Saputra, T. M., Hernadewita, H., Prawira Saputra, A. Y., Kusumah, L. H., & ST, H. (2019). Quality improvement of molding machine through statistical process control in plastic industry. *Journal of applied research on industrial engineering*, *6*(2), 87-96.

[13] Sunadi, S., Purba, H. H., & Saroso, D. S. (2020). Statistical Process Control (SPC) method to improve the capability process of drop impact resistance: a case study at aluminum cans manufacturing industry in Indonesia. *Journal of applied research on industrial engineering*, *7*(1), 92-108.

[14] Calzada, M. E., & Scariano, S. M. (2003). Reconciling the integral equation and Markov chain approaches for computing EWMA average run lengths. *Communications in statistics-simulation and computation*, *32*(2), 591-604.

[15] Petcharat, K., Areepong, Y., & Sukparungsee, S. (2013). Exact solution of average run length of EWMA chart for MA (q) processes. *Far East journal of mathematical sciences*, *78*(2), 291.

[16] Woodall, W. H., & Mahmoud, M. A. (2005). The inertial properties of quality control charts. *Technometrics*, *47*(4), 425-436.

[17] Capizzi, G., & Masarotto, G. (2010). Combined Shewhart–EWMA control charts with estimated parameters. *Journal of statistical computation and simulation*, *80*(7), 793-807.